

Imaging of Cerebrospinal Fluid Rhinorrhea and Otorrhea



Mahati Reddy, MD, Kristen Baugnon, MD*

KEYWORDS

- CSF leak • Idiopathic intracranial hypertension (IIH) • Skull base fractures • Cisternogram

KEY POINTS

- Any clinically suspected cerebrospinal fluid (CSF) rhinorrhea or otorrhea should first be confirmed with testing for β 2-transferrin, a protein specific to the CSF.
- High-resolution computed tomography (CT) imaging through the sinuses and mastoids should be the first step to diagnose the possible site of a CSF leak.
- CT cisternogram can be helpful to confirm the site of a leak in patients with multiple osseous defects on CT and an active leak.
- Magnetic resonance cisternogram is helpful in patients with intermittent leaks or suspected meningoencephaloceles.
- Morphologic features suggesting underlying idiopathic intracranial hypertension should be mentioned on imaging of suspected CSF leak, because this can alter the patient's management.

INTRODUCTION

A skull base cerebrospinal (CSF) leak or fistula is an abnormal communication of the sterile subarachnoid space with the sinonasal or tympanomastoid cavities, and presents clinically with clear rhinorrhea or otorrhea, caused by the presence of both an osseous and a dural defect. The flora of the sinonasal cavity and the middle ear create a conduit for the spread of infection that often results in meningitis, with an approximately 19% lifetime risk of meningitis in patients with persistent CSF rhinorrhea.¹ Despite advances in antibiotic therapy, mortality from bacterial meningitis in adults remains up to 33%, with severe morbidity among survivors, including seizure disorders, encephalopathy, and cranial nerve deficits.² The high risk of life-threatening complications underscores the importance of early detection, accurate diagnosis, and timely repair

of CSF leaks. Endoscopic approaches to CSF leak repair are replacing open transcranial and transfacial methods because of similar rates of success, with significantly lower complication rates of wound infection, sepsis, and meningitis.^{3,4} Especially in the setting of an endoscopic repair, a thorough radiologic investigation is imperative to determine the precise location of the fistula, define the dimensions of the osseous defect, and evaluate the subjective anatomy of the area. This process enables surgeons to plan the surgical approach, graft, and closure technique, and to avoid an open craniotomy.⁵

Not only is imaging essential in determining the site of a CSF leak but it can also aid in determining the underlying cause. CSF leaks can be traumatic or nontraumatic, with most nontraumatic leaks seen in the setting of idiopathic intracranial hypertension (IIH), also known as spontaneous leaks.^{6,7} This article begins with a description of imaging

Disclosure: None.

Department of Radiology and Imaging Sciences, Emory University School of Medicine, Emory University Hospital, 1364 Clifton Road Northeast, Atlanta, GA 30322, USA

* Corresponding author.

E-mail address: kmlloyd@emory.edu

Radiol Clin N Am 55 (2017) 167–187

<http://dx.doi.org/10.1016/j.rcl.2016.08.005>

0033-8389/17/© 2016 Elsevier Inc. All rights reserved.

techniques used to diagnose and characterize the site of a CSF leak and then details the pathophysiology and associated imaging findings in traumatic and spontaneous leaks. In addition, it discusses some challenges in the diagnosis of initial and recurrent leaks with an emphasis on information that is most consequential to referring surgeons.

IMAGING PROTOCOLS

The first diagnostic study to evaluate a patient with CSF rhinorrhea or otorrhea and suspected CSF leak is testing a sample of the fluid for β 2-transferrin, a protein specific to the CSF, because this is the most reliable confirmatory test for a CSF leak.⁸ As discussed previously, rhinorrhea can be a sign of a defect along either the paranasal sinuses or mastoids. Frank otorrhea draining from the external auditory canal in the setting of a tegmen defect within the middle cranial fossa is rare, unless there is a perforation of the tympanic membrane (ie, in the setting of trauma), or a tympanostomy tube. Various methods of testing for β 2-transferrin report sensitivities of 87% to 100% and specificities of 71% to 94%.⁹ Patients with intermittent leaks may be able to collect an adequate volume of sample themselves over the course of a week, if necessary, without storage restrictions to prevent protein degradation.¹⁰ Although not widely used in the United States, beta trace protein is another CSF marker, and some recent studies report that it has a higher sensitivity and specificity than β 2-transferrin with lower cost and faster turnaround time.^{9,11,12} Once the leak is confirmed, localization and characterization can be achieved with radiologic evaluation.

COMPUTED TOMOGRAPHY

High-resolution CT (HRCT) of the paranasal sinuses and mastoids should be the first line of imaging because computed tomography (CT) is the best modality to delineate osseous anatomy with the greatest spatial resolution to pinpoint a site of bony dehiscence. HRCT has a reported sensitivity of 88% to 95% in identifying the site of skull base defect after the presence of CSF leak is confirmed by β 2-transferrin analysis.^{13–16} In a single retrospective study at our institution, CT correctly predicted the site of leak in 100% of the cases when 0.625-mm axial images were available and multiplanar reformations could be generated.¹⁷ In addition to excellent accuracy, HRCT provides unparalleled delineation of the remaining osseous sinonasal anatomy for surgeons to plan their

operative approach and allows the use of an intraoperative image guidance system.¹⁸ Patients should be scanned with multidetector row CT in the supine position with a field of view to include the paranasal sinuses and temporal bones. Continuous thin-section axial images of submillimeter (ie, 0.625 mm) collimation (volumetric) should be reconstructed in the bone algorithm, and sagittal and coronal reconstructions of the raw data should be performed.^{17,19} One of the greatest strengths of HRCT in the evaluation of CSF leak is that an active leak does not need to be present at the time of imaging to be able to identify an osseous defect. However, if the patient has multiple osseous defects, it can be challenging to determine which defect is the definite source of the CSF leak, because the presence of an osseous defect is not always associated with a concomitant dural dehiscence. However, if only 1 osseous defect is identified and the location of the suspected leak on imaging corresponds with the clinical symptoms, no additional imaging is needed, and the patient can proceed to surgical repair.²⁰

Computed Tomography Cisternography

Contrast-enhanced CT cisternography (CTC) is performed by instilling intrathecal nonionic myelographic iodinated contrast and scanning the sinuses in the prone and supine positions, with supine images also obtained before contrast injection for the purposes of comparison. In a positive study, there is extracranial fluid or soft tissue density adjacent to an osseous defect showing 50% or greater increase in Hounsfield units on the post-contrast scan compared with the precontrast scan, suggestive of interval contrast pooling. When introduced in 1977, CTC was considered the study of choice to evaluate CSF fistulae, but it is now selectively used as a problem-solving tool in specific scenarios, primarily in the setting of multiple osseous defects on CT, to determine the site of leak.^{21,22} CTC has a wide range of reported sensitivities of 33% to 100% and specificity of approximately 94%.^{8,13,23–25} The main limitation of CTC is that patients have to be actively leaking, or able to elicit a leak, at the time of examination. Low rates of sensitivity are predominantly attributed to imaging in the absence of an active leak, with other potential causes being obscuration of small leak in the setting of high-density contrast media adjacent to high-density bone and high viscosity of contrast media prohibiting leakage through a fistulous tract.^{25,26} The disadvantages of CTC include high radiation dose related to multiple scans, inherent risk of a lumbar puncture, and potential adverse outcome from iodinated contrast.

Magnetic Resonance Cisternogram

Magnetic resonance (MR) cisternography (MRC) is performed by acquiring heavily T2-weighted (T2w) images to increase conspicuity of the contrast between CSF and the adjacent skull base. The spatial resolution of HRCT is far superior to that of MR imaging, but the advent of three-dimensional (3D)- fast spoiled gradient echo facilitated obtaining thin-slice images that can be reformatted into multiple planes, significantly improving MR imaging of the skull base. Nevertheless, MRC should continue to be used in conjunction with HRCT because MR imaging cannot provide the exquisite osseous detail of CT.^{13,16,27} In a positive study, a CSF column is seen from the subarachnoid space communicating with the extracranial space with or without herniation of meninges and/or brain parenchyma. Sensitivity of these findings on MRC for identifying the site of leak is reported to be up to 94%.²⁸ The added benefit of MR imaging is improved soft tissue contrast that can characterize the contents of tissue herniating through an osseous defect in the setting of possible meningoencephaloceles.

Contrast-Enhanced Magnetic Resonance Cisternogram

Contrast-enhanced MRC is a technique in which intrathecal gadolinium is administered through a lumbar puncture and, subsequently, thin-section T1-weighted sequences are obtained in multiple planes. These sequences can be obtained immediately (1–2 hours after injection of contrast), and in a delayed fashion up to 24 hours after contrast administration if necessary. Similar to a CTC, a positive study shows leakage of contrast medium through dural disruption and adjacent osseous defect, and, similar to noncontrast MR imaging cisternogram, this study also requires HRCT for interpretation. Studies have shown enhanced sensitivity for detection of CSF leaks using this method compared with CT and standard MRC,^{14,25,29} particularly in the setting of slow flow or intermittent leaks, a population that is difficult to diagnose with CTC, possibly in part due because of the ability to perform delayed imaging up to 24 hours later.³⁰ This technique has been reported to be up to 100% sensitive for high-flow leaks, and up to 60% to 70% sensitive for slow-flow leaks.³¹ Additional potential benefits of this technique include the lack of ionizing radiation, the ability to assess for meningoceles at the time of the examination, and the ease of interpretation compared with CT cisternogram caused by the improved differentiation of contrast and bone. However, note that intrathecal administration of

gadolinium is not yet approved by the US Food and Drug Administration (FDA), although it has been used safely at low doses (0.05 mmol) for several years throughout the world in selected patients.^{29,32,33} Although long-term studies are still pending, a single study following 107 patients for an average of 4.2 years showed no long-term adverse effects related to the gadolinium administration.³⁴ However, given the invasive nature of the study, the known neurotoxicity of gadolinium in high doses, and current off-label use, selective use of this technique as a problem-solving tool is prudent,⁸ particularly in patients with renal failure.³⁵ At our institution, this is included in the algorithm only in selected patients with normal renal function, inability to obtain fluid to test for β 2-transferrin, and very high clinical suspicion, and is obtained only after thorough off-label use consent.

Radionuclide Cisternography

Radionuclide cisternography (RNC) is a nuclear medicine diagnostic examination in which a radio-tracer (technetium-99 or indium-111) is injected intrathecally, then several pledges are placed throughout the nasal cavity. After 24 to 48 hours, the radioactivity is measured in each pledge to confirm the presence of a CSF leak⁸ and compared with baseline serum levels. A ratio of 2:1 or 3:1 is considered a positive study. Theoretically, some localization information could be obtained by corroborating locations of the radioactive pledges to their precise location in the nasal cavity. However, anecdotal experience suggests that accurate localization is extremely limited, because the intranasal pledges are not well tolerated by patients and often move, secretions can mix from side to side, and (as discussed previously) leaks within the middle ear may present with CSF in the nasal cavity through the eustachian tube. Additional disadvantages of RNC include the invasive nature of the study, high cost, and moderate accuracy.⁸ In general, it is typically reserved only for rare problem-solving cases to confirm the presence or absence of a leak, and is not included in our standard imaging algorithm.

Fig. 1 shows our recommended imaging algorithm for patients with suspected skull base CSF leak. Our protocols for CT, CT, and MRC with and without intrathecal gadolinium are summarized in **Table 1**.

PATHOLOGY AND IMAGING FINDINGS

The imaging appearance of CSF leaks often depends on the underlying cause. As described

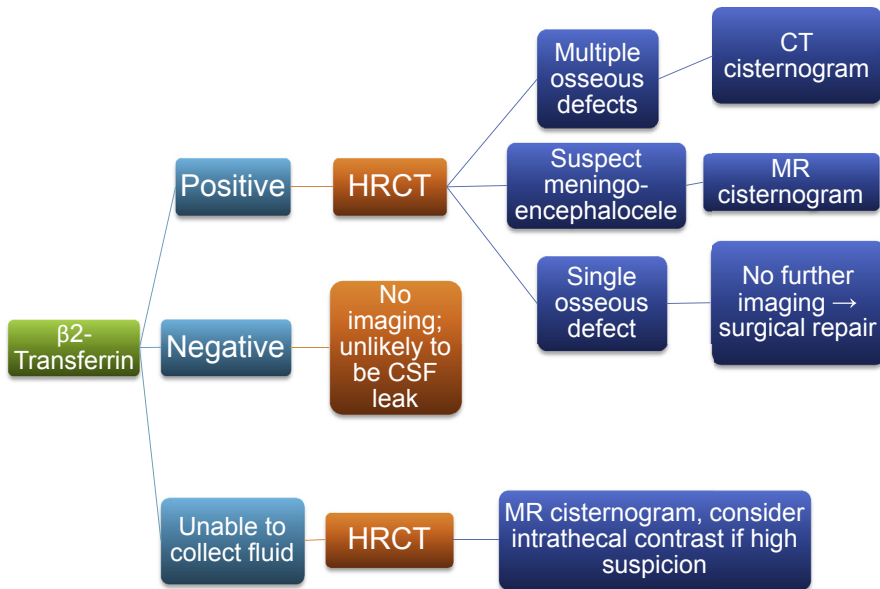


Fig. 1. Imaging algorithm for patient with suspected CSF leak.

earlier, CSF leaks can be classified as traumatic or nontraumatic, with the traumatic leaks resulting from either accidental or iatrogenic trauma, and the nontraumatic leaks are either secondary, caused by underlying tumor or congenital disorder, or spontaneous (without history of prior trauma, surgery, tumor, or congenital lesion).

Traumatic Leaks

Traumatic leaks, including both accidental and iatrogenic leaks, are still the most commonly encountered type of CSF leak, reportedly accounting for up to 80% to 90% of CSF leaks in older literature,³⁶ although spontaneous leaks are increasing in frequency, as discussed later.

Accidental trauma

Approximately 10% to 30% of skull base fractures are complicated by CSF leaks, particularly those that are comminuted and extend through the anterior cranial fossa, likely because of the tightly adherent dura in a region of inherently thin cribriform plates and ethmoid roofs. However, frontobasal fractures that extend through the posterior table of the frontal sinus, central skull base fractures extending through the sphenoid sinus, and temporal bone fractures extending through the tegmen can also result in CSF rhinorrhea or otorrhea.³⁷

Imaging findings include a nondisplaced or comminuted fracture extending through the skull base, and often the presence of pneumocephalus (**Fig. 2**). Pneumocephalus in the traumatic setting

should imply a skull base fracture and dural defect, and, if seen, careful attention to the areas described earlier should be undertaken to exclude the possibility of even a subtle or occult skull base fracture (**Fig. 3**).

Most patients (80%) present with CSF rhinorrhea or otorrhea in the first 48 hours, and 95% of patients present by the first 3 months after trauma.³⁸ The initial delay in presentation is likely caused by the resolution of hemorrhage initially sealing the defect, combined with increased activity as the patient heals and rehabilitates. However, a small subset of patients present in a very delayed fashion, months or years after the trauma, presumably due to atrophy of granulation tissue, or possibly because of bony fragments slowly eroding the dura over time. However, although CSF leaks are fairly common in the setting of complex skull base trauma, they rarely require treatment, because up to 85% of patients CSF leaks heal spontaneously with conservative management, including bed rest, avoiding Valsalva (ie, stool softeners), and occasionally lumbar drain placement for persistent leaks.^{37,39} However, persistent leaks do necessitate repair; one study of 160 patients with traumatic leak showed a 1.3% chance of meningitis per day for the first 2 weeks after the trauma, which increased to 7.4% per week for the first month, 8.1% per month for the first 6 months, and 8.4% per year from then onward.⁴⁰ When patients require repair in the early posttraumatic period, the site of the leak is usually obvious and rarely a diagnostic dilemma, therefore

Table 1**Suggested imaging protocols for patients with suspected CSF leak**

CT Paranasal Sinuses Without Contrast			
1	Scout	Tip of nose to back of mastoid	
2	Axial bone thin	0.625 mm (or 0.6 mm)	
3	Axial soft	2.5 mm (or 3 mm)	
4	Coronal bone	0.625 mm (or 0.6 mm)	
5	Sagittal bone	0.625 mm (or 0.6 mm)	
CT Cisternogram (CT Paranasal Sinuses Without and with Intrathecal Contrast)			
1	Scout	Tip of nose to back of mastoid	
2	Axial bone thin	Supine helical; 0.625 mm (or 0.6 mm)	
3	Axial soft	2.5 mm (or 3 mm) reconstructed	
4	Coronal bone	0.625 mm (or 0.6)	
5	Sagittal bone	0.625 mm (or 0.6)	
<i>Patient to fluoroscopic suite for 5–7 mL of intrathecal iodinated myelographic contrast</i>			
<i>Before placing patient on CT table, head hanging/provocation techniques</i>			
6	Scout	Tip of nose to back of mastoid	
7	Coronal bone prone	Prone (detail, direct coronal); 0.625 mm	
8	Axial bone thin	Supine; 0.625 mm	
9	Axial soft postspine	2.5 mm (reconstructed)	
10	Coronal bone	0.625 or 0.6 mm (reconstructed from supine post data set)	
11	Sagittal bone	0.625 or 0.6 mm (reconstructed from supine data set)	
MR Cisternogram: MR Brain Without and with IV Contrast			
#	Sequence	Plane	Comment
1	T1	Sagittal	Brain
2	T2 FLAIR	Axial	Brain
3	T1	Axial	Top of frontal sinus to tip of clivus (3 mm)
4	T1	Coronal	Tip of nose to back of mastoid (3 mm)
5	3D T2 SPACE	Coronal	Tip of nose to back of mastoid (1 mm)
6	T2	Coronal	Tip of nose to back of mastoid (3 mm)
<i>Administer IV contrast</i>			
7	T1 fat-saturated postcontrast	Axial	Top of frontal sinus to tip of clivus (3 mm)
8	T1 fat-saturated postcontrast	Coronal	Tip of nose to back of mastoid (3 mm)
Gadolinium-Enhanced MR Cisternogram (MR Brain Without and with Intrathecal Contrast)			
#	Sequence	Plane	Comment
1	T1	Sagittal	Brain
2	T2 FLAIR	Axial	Brain
3	T2 SPACE	Coronal	Tip of nose to back of mastoid (1 mm)
4	T1 fat-saturated (VIBE)	Axial	Top of frontal sinus to tip of clivus (1 mm)
5	T1 fat-saturated (VIBE)	Coronal	Tip of nose to back of mastoid (1 mm)
6	MPRAGE	Coronal	Tip of nose to back of mastoid (1 mm)
<i>Patient to fluoroscopic suite for administration of intrathecal contrast: 0.5 mL of gadopentetate Dimeglimine diluted in 5 mL of CSF, injected slowly, rescanned 1–2 h later, ± again in 4–24 h</i>			
7	T1 fat-saturated (VIBE) postcontrast	Axial	Top of frontal sinus to tip of clivus (1 mm)
8	T1 fat-saturated (VIBE) postcontrast	Coronal	Tip of nose to back of mastoid (1 mm)
9	MPRAGE postcontrast	Coronal	Tip of nose to back of mastoid (1 mm)

Abbreviations: FLAIR, fluid-attenuated inversion recovery; IV, intravenous; MPRAGE, magnetization-prepared rapid gradient echo; SPACE, sampling perfection with application optimized contrasts using different flip angle evolutions, siemens 3D T2 TSE sequence; VIBE, volume interpolated breathhold examination, 3D spoiled turbo gradient echo with fat saturation.



Fig. 2. (A, B) Axial CT images showing a comminuted complex frontobasal fracture extending through the frontal sinuses and anterior cranial fossa, resulting in traumatic CSF leak with pneumocephalus (arrow in B).

often only HRCT should be required preoperatively for surgical planning.⁴¹ However, full radiologic evaluation and work-up can be necessary for those patients who present in a delayed fashion (**Fig. 4**).

Iatrogenic leaks

Iatrogenic CSF leaks can occur as a result of neurosurgical or otolaryngologic procedures along the skull base, and reportedly account for about 16% of cases of traumatic rhinorrhea.⁴² Endoscopic endonasal approaches to skull base tumors, including pituitary or clival tumors, have significantly increased in frequency over the last decade, and CSF leaks are a known potential complication of this approach, reportedly occurring in up to 13.8% of patients in one study.⁴³ Most iatrogenic leaks occur in the first 2 postoperative weeks; resolve spontaneously or with lumbar drain placement; and, if they do require repair, typically only require HRCT for preoperative planning, because the site of the leak should be

obvious (the site of the prior surgery) (**Fig. 5**). Postoperative changes with packing and blood products make CTC challenging in the early postoperative setting.

Postoperative CSF leaks can complicate craniotomies that inadvertently extend through the frontal sinus or mastoid air cells (**Fig. 6**), as well as those in which clinoidectomies are performed for exposure to the parasellar region, such as aneurysm clipping, if the patient's pneumatization of the sphenoid sinus extends into the clinoid process, which is a variant occurring in nearly one-third of the population (**Fig. 7**).⁴⁴ The risk of CSF leak after anterior clinoidectomy is reportedly up to 2% to 7%.⁴⁵ For this reason, any pneumatization of the clinoid process should be mentioned on preoperative CT angiography, particularly if the patient has a periclinoid aneurysm (**Fig. 8**).⁴⁶

In addition, CSF leaks are a known potential complication of endoscopic sinus surgery, with the risk increasing in the setting of revision surgery or sinonasal polyposis, when the surgical

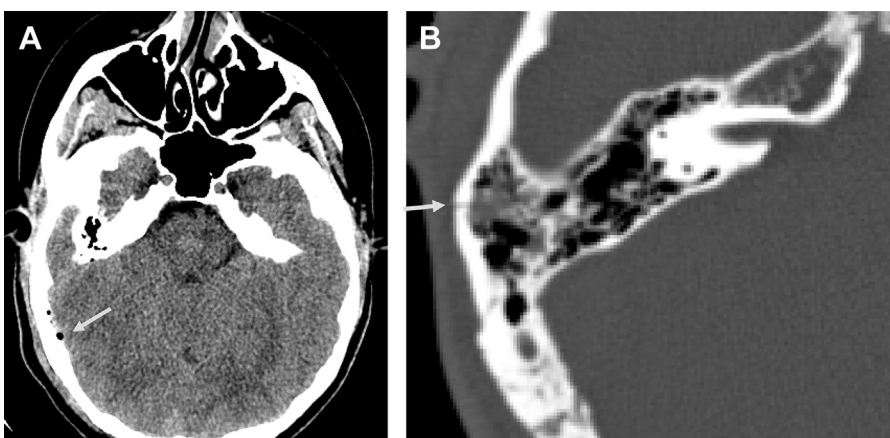


Fig. 3. (A) Axial CT image shows mild soft tissue swelling and subtle focus of pneumocephalus (arrow) along the right temporal lobe. (B) Temporal bone CT image with a subtle linear nondisplaced defect in the right mastoid air cells (arrow).

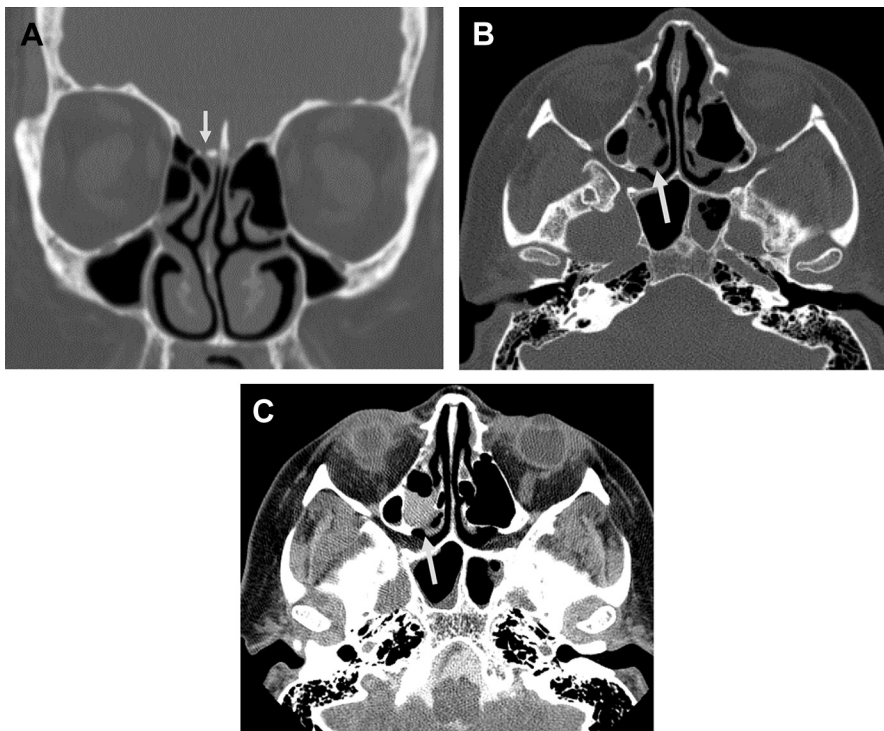


Fig. 4. A 42-year-old woman presenting with β 2-transferrin-positive right-sided rhinorrhea. History of trauma 4 years previously. (A) Coronal CT bone window images show focal sclerosis along the right cribriform plate with dehiscence of the lateral lamella (arrow). The patient had an additional bony defect in the sphenoid sinus (not shown), and therefore underwent CTC. (B) Axial precontrast image shows opacification of a single right posterior ethmoid air cell (arrow) just posterior to the defect shown in A. (C) Postcontrast axial CT image (soft tissue window) shows increased density within the opacified cell, diagnostic of the site of the CSF leak (arrow).

landmarks are distorted. Using image guidance has been shown to reduce the risk significantly, is indicated in these complex settings, and has reduced the risk of CSF leak after endoscopic

sinus surgery to reportedly only 0.5%.⁴² Most of these iatrogenic leaks can be seen along the vertical insertion of the middle turbinate, at the thin cribriform plates and lateral lamella; however,

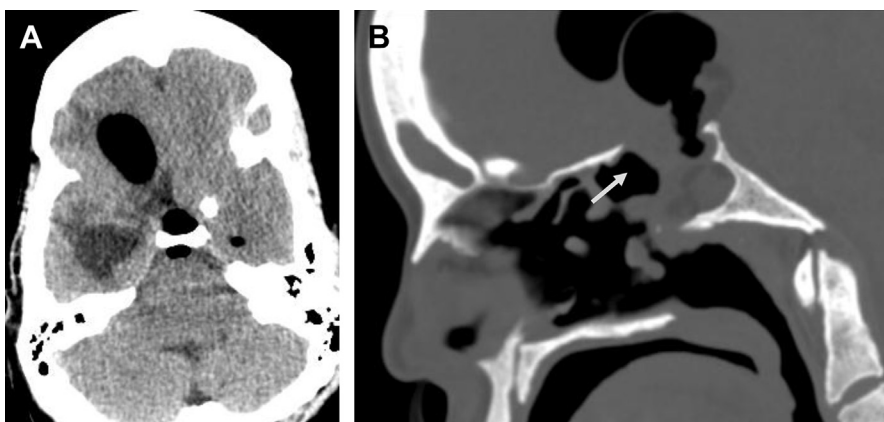


Fig. 5. A 22-year-old woman presents with headaches, lethargy, and rhinorrhea 3 weeks after transphenoidal approach for resection of craniopharyngioma. (A) Axial noncontrast head CT showing air within the suprasellar cistern, pneumocephalus within the prepontine cistern, and significant intraventricular air with hydrocephalus. (B) Sagittal reformat of preoperative sinus CT showing the large skull base defect and graft at the site of the prior surgery (arrow).

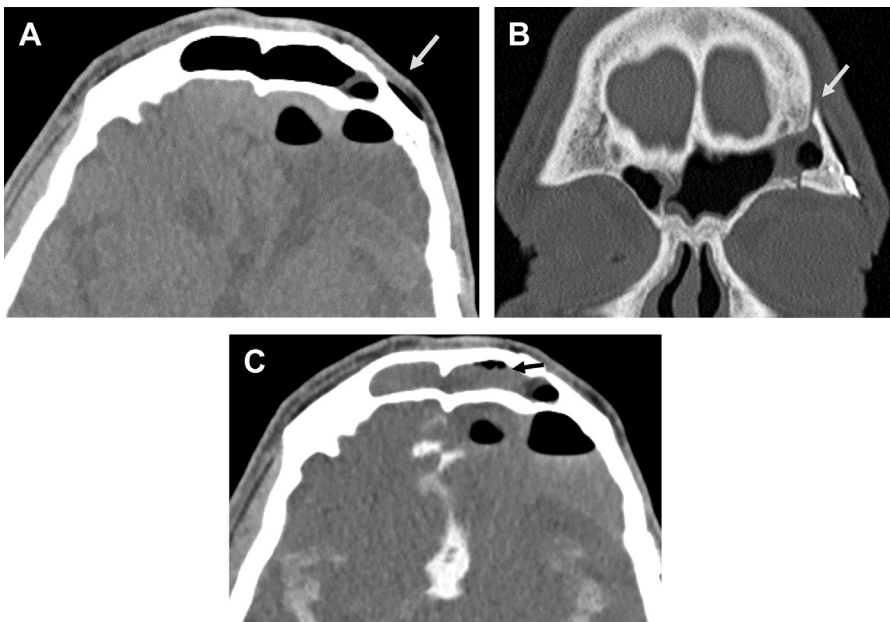


Fig. 6. A 59-year-old patient after craniotomy for sphenoid wing meningioma resection. (A) Axial precontrast CT cisternogram images showing a large air-filled and fluid-filled extra-axial collection, as well as an air bubble seen laterally in the left frontal sinus, and subcutaneous gas at the craniotomy site (arrow). (B) Coronal bone window reformatted precontrast images show the craniotomy extending through the lateral aspect of the frontal sinus (arrow). (C) Axial postcontrast CT cisternogram images showing contrast filling the frontal sinus with a fluid level, indicates an active leak (black arrow).

other common sites of injury include the posterior ethmoid roof, sphenoid sinus, and posterior table of the frontal sinus (**Fig. 9**).⁴⁷

Nontraumatic Leaks

Secondary leaks

The least commonly encountered category of CSF leaks are those nontraumatic leaks in which a

definite pathologic cause is identified. These leaks can be caused by erosion of the skull base by tumors (before or after radiation therapy), mucocles, osteonecrosis, or other erosive processes (eg, Gorham-Stout disease) (**Fig. 10**). CSF leaks can also be caused by congenital lesions, which can occur with or without increased intracranial pressure. The congenital lesions reported to cause

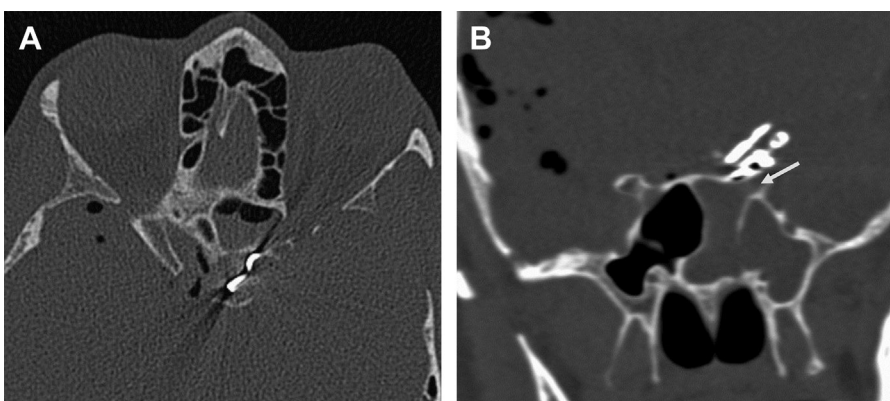


Fig. 7. A 48-year-old woman after craniotomy with clinoideectomy for periclinoid aneurysm clipping presenting with headache and rhinorrhea 1 week postoperatively. Axial (A) and coronal (B) bone window images of HRCT of the sinuses showing postoperative changes after clinoideectomy and aneurysm clipping with fluid level in the left sphenoid sinus and worsening pneumocephalus, indicating CSF leak. Note the fluid within the previously pneumatized optic strut adjacent to the aneurysm clip (arrow in B).

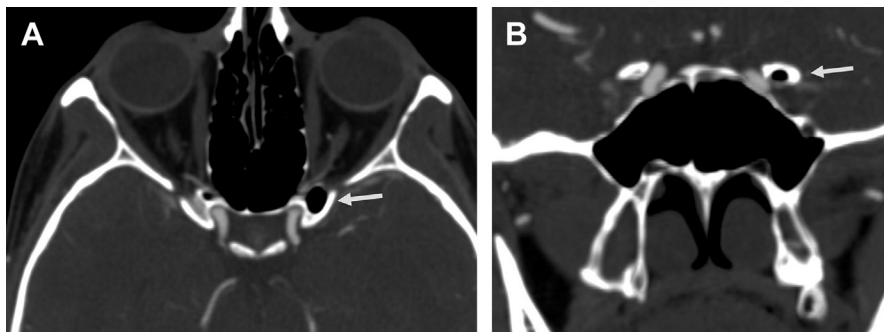


Fig. 8. Axial (A) and coronal (B) CT angiogram images performed to assess an aneurysm (not shown) showing a pneumatized left clinoid process (arrow). These processes should be mentioned in the report, particularly if ipsilateral to a periclinoid aneurysm.

CSF leak include congenital encephaloceles, persistent craniopharyngeal canal (with or without tumor) (Fig. 11), or congenital widening of the dia-phragma sella (primary empty sella syndrome).⁴⁸

Spontaneous leaks

Spontaneous leaks are those leaks without an underlying lesion, congenital abnormality, or history of trauma or surgery, and most of these are thought to be caused by underlying IIH. IIH is a headache syndrome classically seen in overweight women, with visual disturbance, papilledema, and sometimes tinnitus or hearing loss. Population studies in the United States performed in late 1980s showed an annual incidence of IIH of approximately 1 in 100,000 in the general population, which increased to 19 in 100,000 in overweight women aged in the range of 20 to 44 years.⁴⁹ There has also been an increased prevalence of this disease over the last few

decades, likely caused by the epidemic of obesity in the United States, as well as increased awareness of IIH among health care professionals. There is a great deal of clinical and radiologic overlap between the findings of patients with IIH and spontaneous CSF leak, which has led to the proposed link between these 2 entities. It is proposed that, in patients with spontaneous CSF leak, increased intracranial pressure, possibly caused by increased intra-abdominal and intravenous pressures, leads to increased dural pulsations, which erode the skull base over time, ultimately leading to a dural tear and CSF leak.^{7,50} In addition to these osteodural defects, this sustained increased pressure can also lead to the formation of prominent arachnoid pits at the skull base with areas of overlying dural thinning, as well as the formation of meningoceles and meningoencephaloceles. As such, spontaneous CSF leaks are emerging as a more frequent presentation of IIH,⁵¹ and are becoming one of the most commonly encountered causes of CSF leak requiring imaging evaluation. Historically, nontraumatic spontaneous leaks have been reported to account for only approximately 4% of CSF leaks. However, more recent data suggest that spontaneous leaks may be more common than was previously considered, ranging from 20.8% to 40% of CSF leaks.^{18,52,53}

Although the International Headache Society does not include imaging findings among the diagnostic criteria for IIH, neurologic imaging is required at the minimum to exclude hydrocephalus, mass, or structural or vascular lesion. Although not highly specific, there are many imaging findings that are suggestive of IIH, especially when seen in combination, and can help prompt additional work-up, including ophthalmologic evaluation and CSF opening pressures.⁵⁴ These indicative findings include empty sella, optic nerve sheath enlargement and/or tortuosity, optic nerve head protrusion with flattening of the posterior

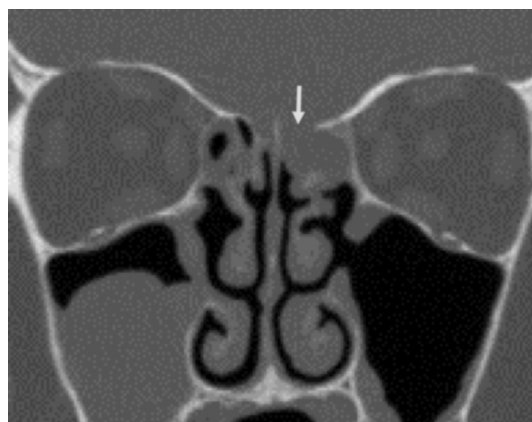


Fig. 9. Coronal bone window CT images showing a large defect along the left cribriform plate, lateral lamella, and ethmoid roof (arrow), with adjacent polypoid nondependent soft tissue (concerning for meningoencephalocele).



Fig. 10. A 22-year-old woman with a history of Gorham disease presenting with headaches and CSF rhinorrhea. Coronal bone window CT images from a CT cisternogram show osteolysis of the right temporal bone, involving the tegmen (arrow). The ipsilateral occipital bone and mandible were also involved.

globe, and optic nerve head edema with enhancement (**Fig. 12**). Findings at the skull base that can also be detected on the HRCT of the sinuses, in addition to the large empty sella include scalloping of the inner table of the calvarium, prominent arachnoid pits, multiple osseous defects along

the skull base, and enlargement of the skull base foramina (**Fig. 13**).^{51,55} The skull base should be interrogated carefully for meningoceles because they are significantly more common in patients with IIH, affecting up to 11% of all patients with IIH in some series,⁵⁶ but are seen in 50% to 100% of patients with spontaneous CSF leak in other series⁵¹ (**Fig. 14**). Bilateral transverse sinus stenosis is also associated with IIH and is seen in these patients, although it is unclear whether this is the cause or result of the underlying disorder (**Fig. 15**). Another recently described finding seen in patients with IIH is low-lying cerebellar tonsils with inferiorly displaced brainstem and cerebellum, mimicking a Chiari 1 malformation.⁵⁷ The most common sites of spontaneous CSF leaks from IIH are the ethmoid roof/cribriform plate and lateral recess of the sphenoid.^{58–60} Because these patients are prone to developing meningoceles and multiple skull base defects,⁶¹ they often require multiple modalities of imaging for their work-up, including MR and CTC.

In the setting of an active CSF leak, patients with IIH may have pseudonormalized intracranial

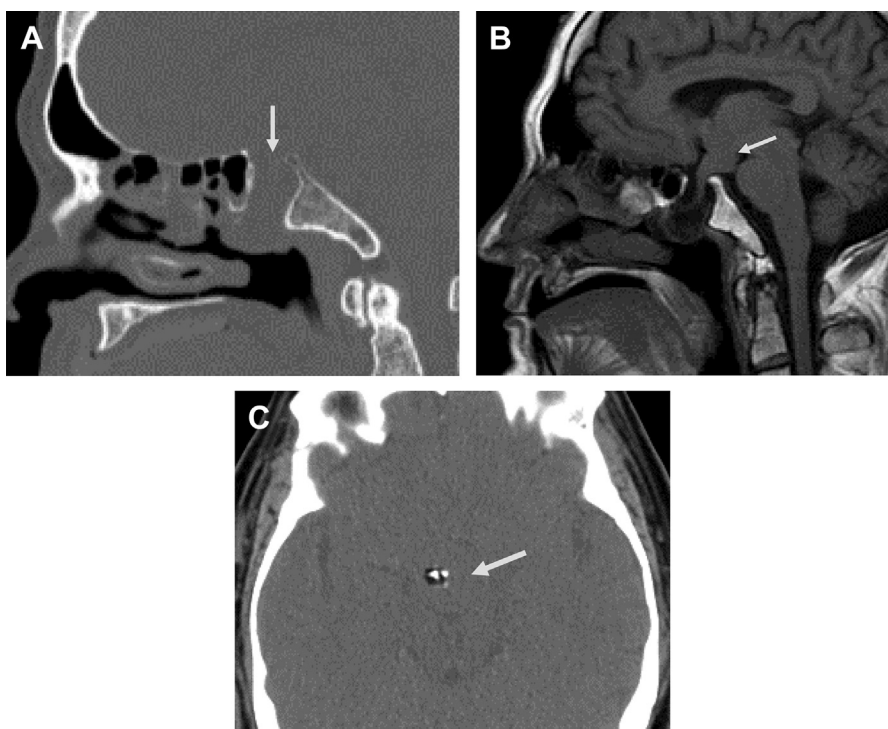


Fig. 11. A 49-year-old man presenting with recurrent meningitis. (A) Sagittal CT images show a large defect in the expected location of the craniopharyngeal canal (arrow), through which there is herniation of polypoid nondependent soft tissue into the nasopharynx. (B) Sagittal T1-weighted MR imaging through the midline shows a large cephalocele herniating through the defect, with herniation of the infundibulum. Note the soft tissue fullness in the expected location of the sella and suprasellar cistern (arrow). (C) Axial soft tissue window CT image showing fat and calcium in the large sellar/suprasellar mass compatible with a teratoma (arrow). This craniopharyngeal canal defect is type 3C,⁶⁹ presenting with recurrent meningitis caused by the large cephalocele.

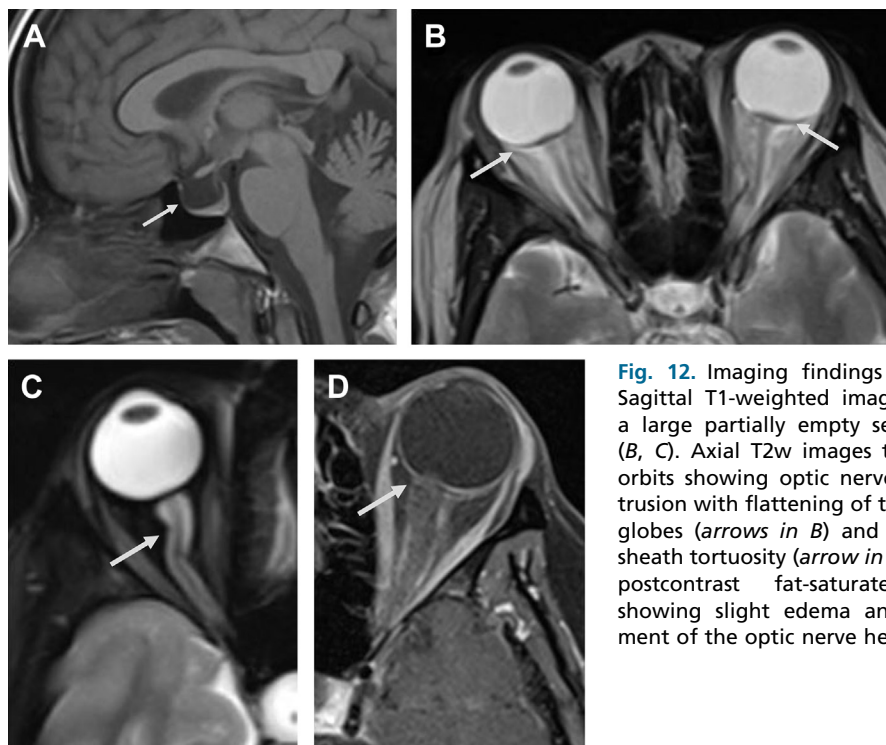


Fig. 12. Imaging findings of IIH. (A) Sagittal T1-weighted images showing a large partially empty sella (arrow). (B, C) Axial T2w images through the orbits showing optic nerve head protrusion with flattening of the posterior globes (arrows in B) and optic nerve sheath tortuosity (arrow in C). (D) Axial postcontrast fat-saturated images showing slight edema and enhancement of the optic nerve head (arrow).

pressure measurement caused by spontaneous decompression, therefore opening pressures may not be helpful at the time of diagnosis. However, the underlying diagnosis of IIH should be suggested if the characteristic imaging features described earlier are present in a patient with a CSF leak. Suggesting the diagnosis prospectively is helpful for the treating surgeon, because these patients have an overall worse prognosis, with increased tendency to recur after treatment, either at the site of initial repair, or frequently at another site of osseous thinning or dehiscence, particularly if their underlying IIH is not addressed. Recurrence rates after repair of idiopathic CSF leaks range from 25% to 87%.^{38,51,62–65} In addition to considering surgical repair, patients with documented or suspected IIH may need to be managed medically via acetazolamide medication, weight reduction strategies, or even ventriculoperitoneal or lumbar-peritoneal shunting, as a last resort.⁵¹

DIAGNOSTIC CRITERIA

Clinical Diagnosis

As discussed earlier, the clinical diagnosis of CSF leak should be confirmed with β 2-transferrin testing of the rhinorrhea or otorrhea, if possible. Endoscopic examination findings of CSF leak

include the presence of clear watery rhinorrhea that pools and increases with Valsalva or provocative head-hanging maneuvers, as well as the possible presence of a blue pulsatile mass, if there is a large meningocele. However, the endoscopic visualization of the site of a leak depends on the variable degree of exposure of the skull base, and, in most circumstances, examination is normal. If the site of a leak is in question, and the patient is presenting with CSF rhinorrhea, one other possible technique for clinical diagnosis is the intrathecal administration of sodium fluorescein, a green dye, in an effort to localize the site of the leak on nasal endoscopy. This fluorescein may be administered preoperatively (often at the time of perioperative lumbar drain placement), to aid the surgeons in diagnosing the leak intraoperatively and/or confirm water-tight closure on repair. However, the false-negative rate of this technique reportedly ranges from 15% to 44%, and the intrathecal use of fluorescein is currently not FDA approved, so this technique is typically reserved for problem-solving cases only.⁶⁶

Imaging Diagnosis

Imaging is essential to localize the site of the leak and aid in preoperative planning. Specific criteria

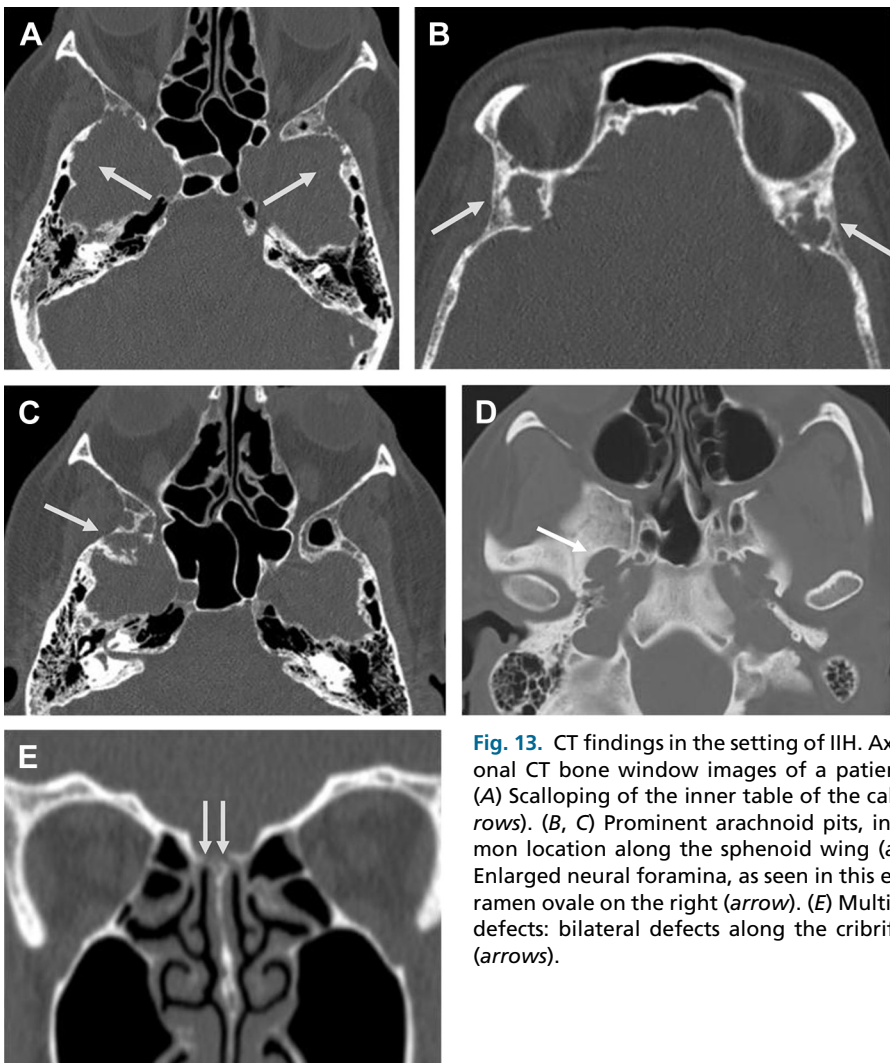


Fig. 13. CT findings in the setting of IIH. Axial and coronal CT bone window images of a patient with IIH. (A) Scalloping of the inner table of the calvarium (arrows). (B, C) Prominent arachnoid pits, in their common location along the sphenoid wing (arrows). (D) Enlarged neural foramina, as seen in this enlarged foramen ovale on the right (arrow). (E) Multiple osseous defects: bilateral defects along the cribriform plates (arrows).

for diagnosing a CSF leak on each of the previously described modalities is as follows:

- CT (**Fig. 16**):
 - Presence of osseous defects in the skull base, particularly if there is adjacent fluid layering dependently within or adjacent to the bony defect in the sinuses or mastoids
 - Polypoid nondependent soft tissue in the sinonasal cavity, or along the tegmen, adjacent to an osseous defect (suspicious for meningoencephalocele)²⁰
 - Particularly nondependent unilateral soft tissue in the olfactory recess in isolation should be suspicious for small meningocoele⁶⁷

- CTC (**Fig. 17**):

- Presence of osseous defects in the skull base, plus
- Increased density or pooling of high-density soft tissue in the sinuses or mastoids adjacent to the defect
- Can measure region of interest (ROI) and compare on the precontrast and postcontrast images: a 2-fold increase in attenuation is diagnostic of a leak²⁰
- Other findings include contrast washout intracranially ipsilateral to a high-flow leak, soufflé effect with increasing density of contrast dependently, and movement of contrast with changes in patient position, confirming an active leak

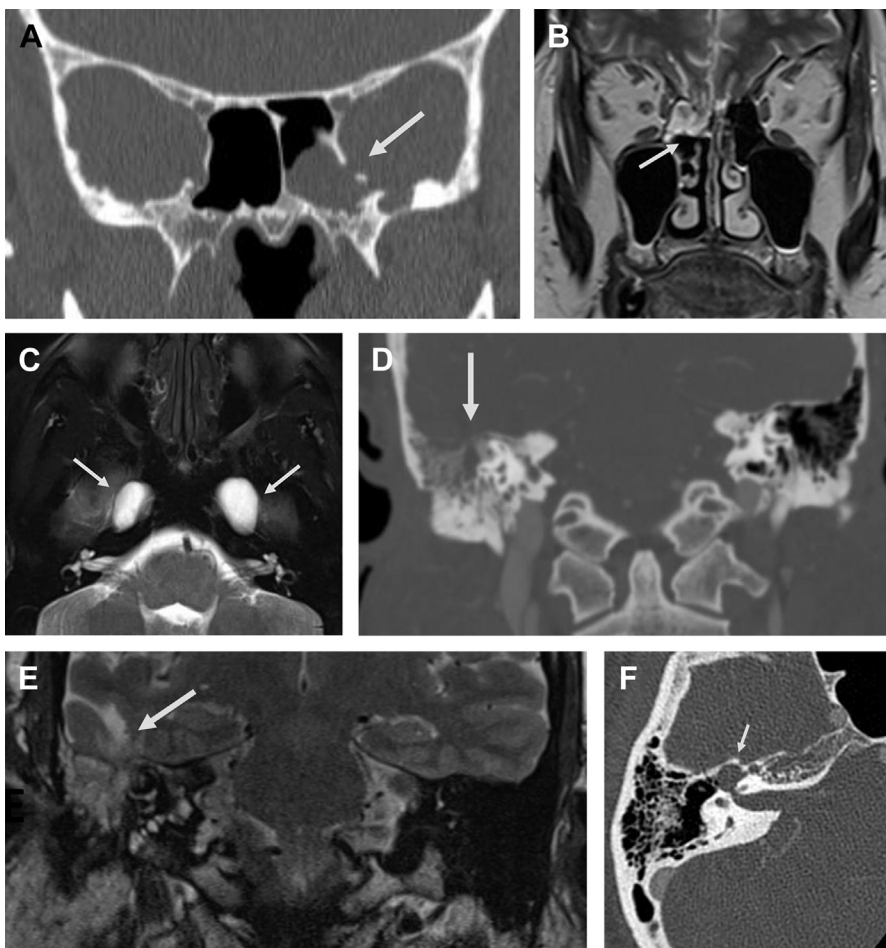


Fig. 14. Images showing the typical appearances and locations of meningoceles in the setting of IIH. (A) CT showing polypoid nondependent soft tissue adjacent to bony defect in the lateral recess of the sphenoid sinus (arrow), adjacent to foramen rotundum. (B) Coronal T2w MR imaging showing herniation of right frontal lobe and CSF into the right ethmoid sinuses (arrow). (C) Axial T2w images showing bilateral Meckel cave meningoceles (arrow). (D, E) Coronal CT and T2w images showing a meningocele along the tegmen mastoideum (arrow). Note the downward tethering of temporal lobe parenchyma and adjacent traction gliosis of the temporal lobe on MR imaging (arrow in E). (F) Polypoid soft tissue and enlargement of the geniculate ganglion (arrow), as commonly seen in facial meningoceles in patients with IIH.

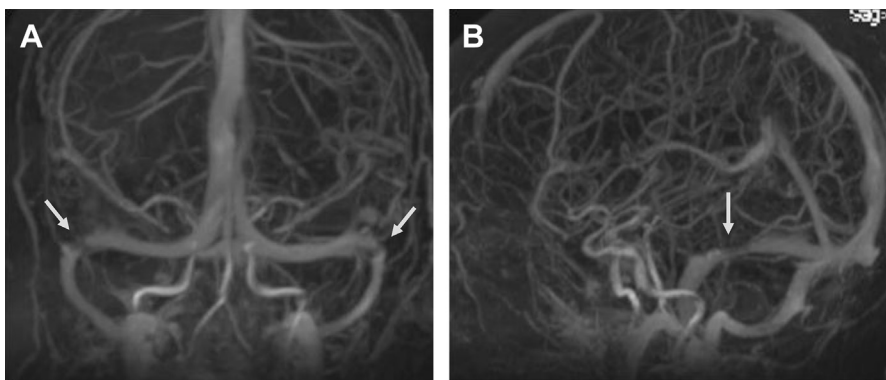


Fig. 15. A 28-year-old woman with IIH. (A, B) Maximal intensity projection reformatted images from MR venography show bilateral high-grade stenosis in the distal transverse sinuses (arrows).

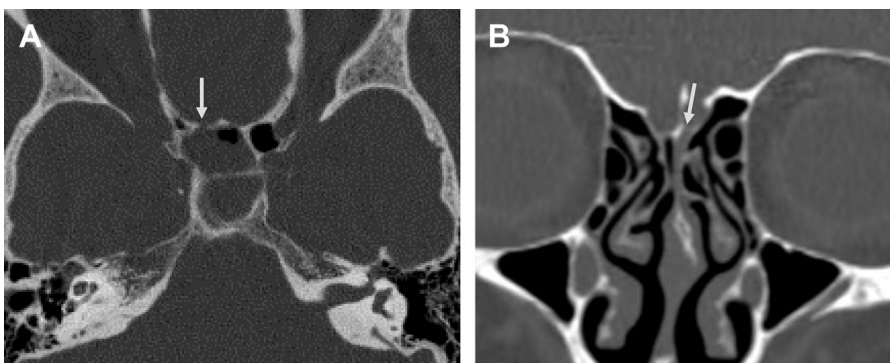


Fig. 16. CT findings of site of CSF leak include osseous defect along the skull base, particularly with fluid/opacification within the adjacent nasal cavity or sinus. (A) Axial CT showing linear defect in the planum sphenoidale and fluid level in the sphenoid sinus (arrow). (B) Coronal CT showing polypoid nondependent soft tissue in the left olfactory recess, suspicious for meningocele (arrow).

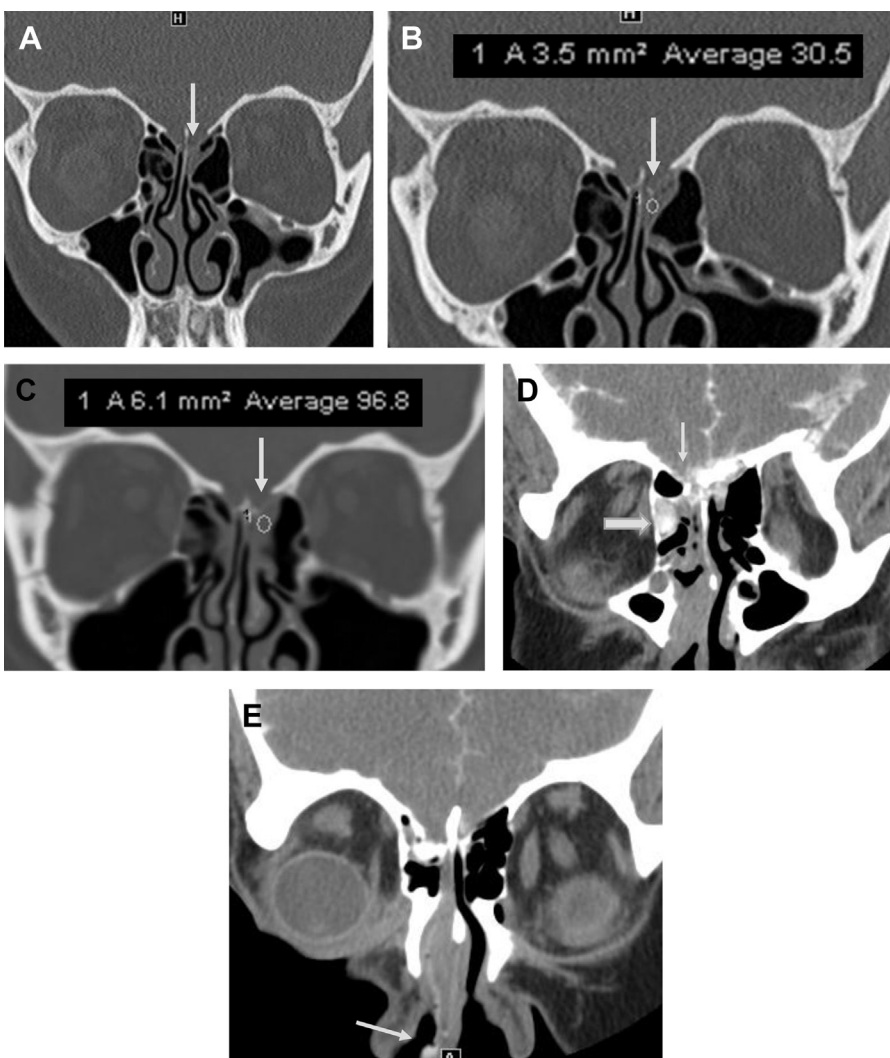


Fig. 17. CT cisternogram findings of CSF leak. (A) Polypoid nondependent soft tissue adjacent to osseous defect in the left olfactory recess, which increases in attenuation from the precontrast (B) to the postcontrast (C) cisternogram images (arrows), confirming the site of leak. (D, E) Direct coronal imaging of another patient in the prone position, showing rapid washout of the CSF intracranially on the side of the leak compared with the other side (arrow in D), as well as the soufflé effect of layering of the dense contrast dependently in a patient with active leak along the right ethmoid roof into the ethmoid sinuses (thick arrow in D). Note also the movement of contrast with changes in patient position, as seen in this patient with contrast trickling anteriorly out of the nose in the prone position (arrow in E).

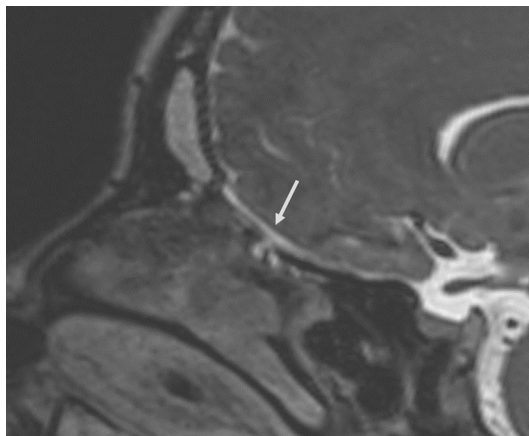


Fig. 18. MR cisternogram findings of CSF leak. Sagittal T2 SPACE sequence image showing a continuous column of CSF extending inferiorly through a defect in the cribriform plate. Note the multiple linear tracts in this complex meningocele along the cribriform plate (arrow).

- MRC (**Fig. 18**):

- Continuous column of T2 hyperintense CSF extending from the subarachnoid space into the sinusal cavity or mastoid/petrous air cells (isointense to CSF on all sequences) through an area of osseous defect (confirmed on prior CT)¹⁴
 - May or may not contain herniated brain contents

- Contrast-enhanced MRC (**Fig. 19**):

- Continuous column of T1 hyperintense gadolinium contrast extending from the subarachnoid space into the sinusal cavity or mastoid/petrous air cells through an area of osseous defect (confirmed on CT)³²

- Helpful to obtain precontrast T1-weighted images for comparison

Differential Diagnosis

There is not much of a differential diagnosis in the setting of a suspected CSF leak. The patient is either leaking CSF or not, and because rhinorrhea or otorrhea could also have benign inflammatory causes, testing the fluid for β 2-transferrin is imperative and confirmatory.

However, a differential diagnosis does exist for a suspected meningocele. Polypoid nondependent soft tissue in the sinusal cavity on CT with an adjacent bony defect could be caused by sinusal polyposis or sinusal neoplasm, thus MR imaging is often necessary to differentiate these entities (**Fig. 20**). In addition, occasionally a skull base cholesteatoma eroding through the tegmen tympani can appear similar to a meningocele extending inferiorly on CT and even routine MR imaging sequences (T2 hyperintense, T1 hypointense, and possibly even peripherally enhancing), but diffusion-weighted sequences should be able to differentiate between those entities, because cholesteatoma should show restricted diffusion (**Fig. 21**).⁶⁸ In addition, spontaneous lateral sphenoid cephaloceles along the greater wing of the sphenoid bone or in the clivus can mimic other skull base neoplasms, such as chordoma or chondrosarcoma (**Fig. 22**), and meningoceles in the region of the geniculate ganglion can mimic other facial nerve tumors such as hemangioma (see **Fig. 14**).⁵⁵ Looking for other morphologic features suggestive of IIH can be helpful, and contrast-enhanced MR imaging confirms the diagnosis. The absence of central enhancement, isointensity to CSF on all sequences, and tethering and/or

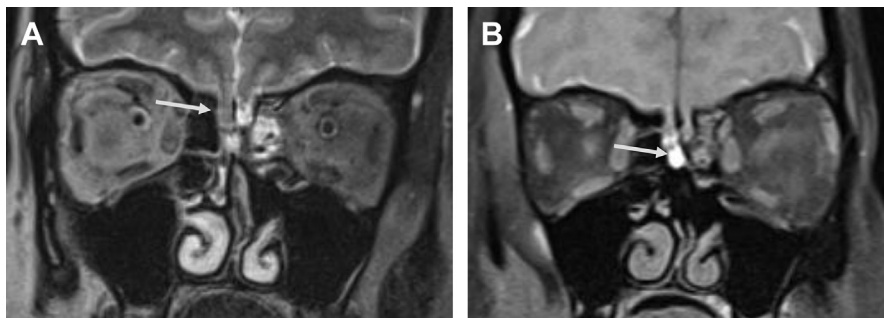


Fig. 19. Contrast-enhanced MR cisternogram findings of CSF leak. (A) Coronal T2w MR images showing T2 hyperintense soft tissue along the superior nasal septum on the right and within the left ethmoid air cells in a patient with intermittent leak and osseous defects adjacent to both sites. However, the right side is most suspicious for meningocele, because there is also tethering/low-lying gyrus rectus on that side (arrow). (B) Coronal T1-weighted (T1w) fat-saturated images from contrast-enhanced MR cisternogram with intrathecal gadolinium, showing filling of a meningocele along the superior nasal septum on the right (arrow), confirming the site of the leak.

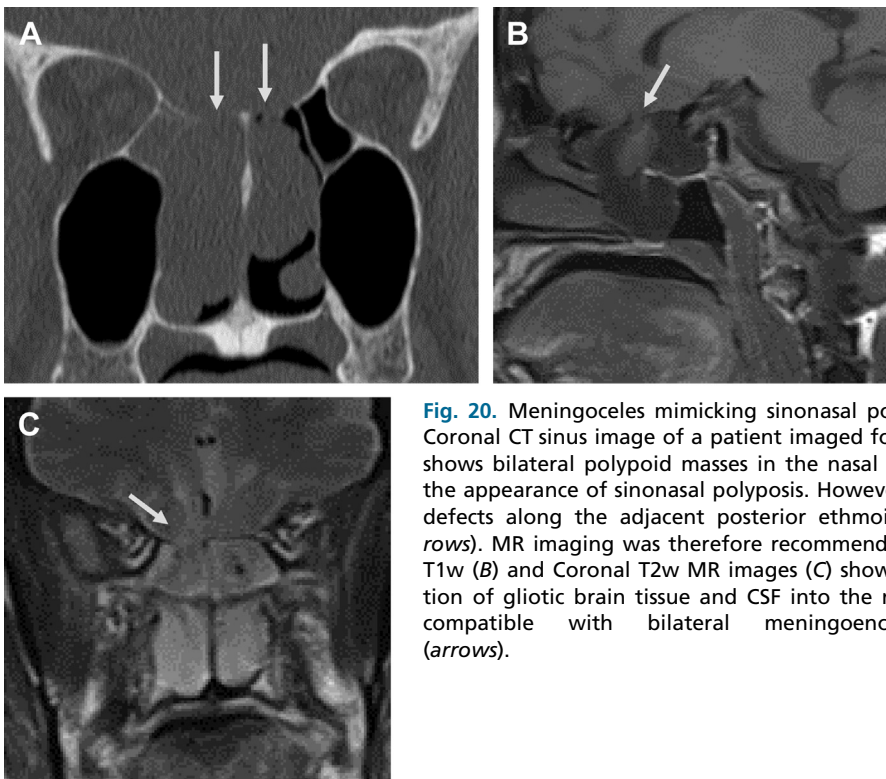


Fig. 20. Meningoceles mimicking sinonasal polyposis. (A) Coronal CT sinus image of a patient imaged for headache shows bilateral polypoid masses in the nasal cavity, with the appearance of sinonasal polyposis. However, note the defects along the adjacent posterior ethmoid roof (arrows). MR imaging was therefore recommended. Sagittal T1w (B) and Coronal T2w MR images (C) showing herniation of gliotic brain tissue and CSF into the nasal cavity, compatible with bilateral meningoencephaloceles (arrows).

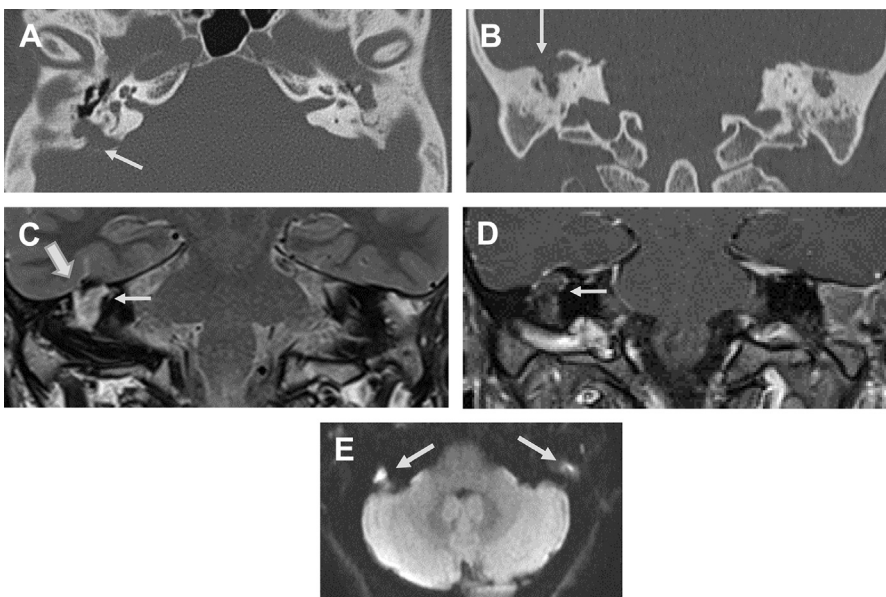


Fig. 21. Cholesteatoma mimicking meningocele. A 21-year-old man with bilateral hearing loss. (A, B) Axial and coronal temporal bone CT shows right-sided soft tissue mass with erosion of the tegmen posteriorly (arrows). Note also the sclerotic underpneumatized mastoid and the left-sided middle ear and mastoid soft tissue mass. (C, D) Coronal T2w and T1w postcontrast fat-saturated sequences showing the right-sided mass to be T2 hyperintense and T1 hypointense with peripheral enhancement (arrows). Note the thinning of the tegmen, but without inferior herniation or tethering of brain parenchyma (thick arrow in C). (E) Axial diffusion-weighted sequences showing diffusion restriction within the mastoid and middle ear masses bilaterally, compatible with cholesteatoma (arrows).

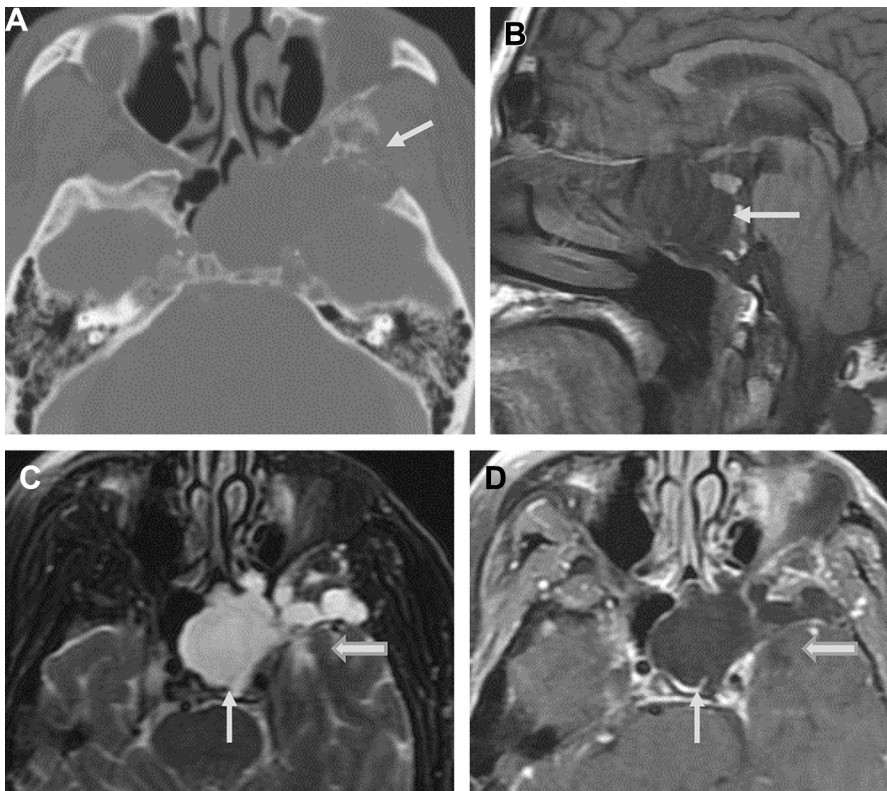


Fig. 22. Sphenoid wing meningocele mimicking skull base neoplasm (ie, chordoma). (A) Axial CT images show expansile lucent mass replacing the left sphenoid wing and clivus, eroding the middle cranial fossa. Note the scalloped appearance often seen with arachnoid pits and meningoceles in the sphenoid wing (arrow). Sagittal T1w (B), axial T2w (C), and axial T1w fat-saturated postcontrast (D) MR images show the lesion to be isointense to CSF on all sequences, without central enhancement, compatible with meningoencephalocele (arrows). Note the tethering and gliosis of the adjacent left temporal lobe (thick arrows in C, D).

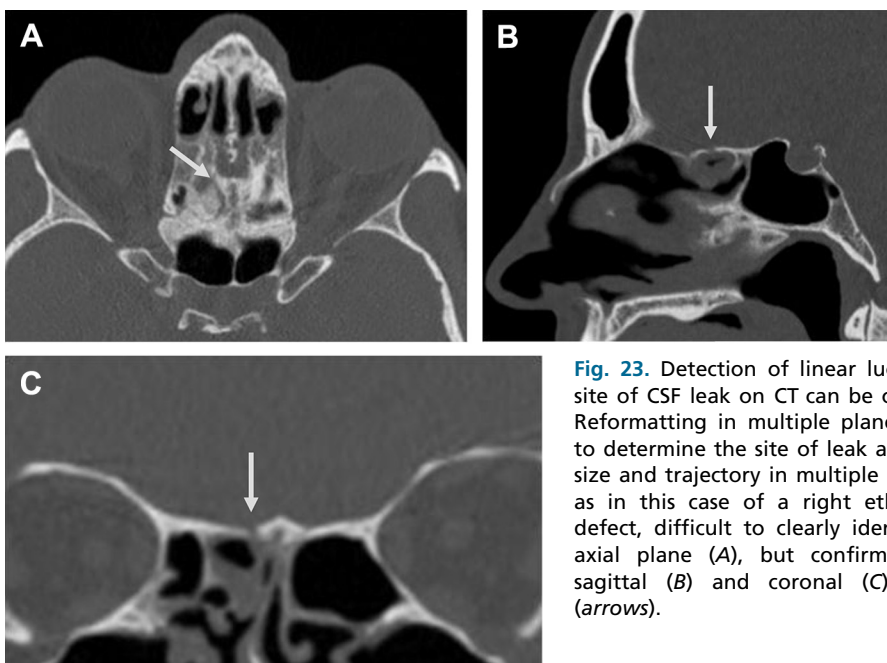


Fig. 23. Detection of linear lucencies and site of CSF leak on CT can be challenging. Reformatting in multiple planes can help to determine the site of leak and show its size and trajectory in multiple dimensions, as in this case of a right ethmoid roof defect, difficult to clearly identify in the axial plane (A), but confirmed on the sagittal (B) and coronal (C) reformats (arrows).



Fig. 24. Patient with right-sided CSF rhinorrhea, positive β 2-transferrin, with subtle lucency along the right cribriform plate and lateral lamella, associated with soft tissue in the right olfactory recess (arrow), which was proved to be the site of the leak intraoperatively.

gliosis of adjacent brain parenchyma, when present, should all suggest a meningocele.

PITFALLS

There are numerous pitfalls and challenges in the complex work-up and evaluation of patients with CSF rhinorrhea and otorrhea. Some of the more frequently encountered include:

- Patients may present with pneumocephalus, middle ear effusion, or meningitis without rhinorrhea, therefore fluid cannot be tested for β 2-transferrin. In this case, a combination of HRCT and MR cisternogram can be helpful to determine a site of a leak, with or without the administration of intrathecal gadolinium.
- Detecting osseous defects on CT can be challenging. Reviewing images on a 3D workstation independently in multiple planes,

magnifying views, and optimizing the window and level settings are all techniques that help to minimize this challenge (Fig. 23).

- Inherent thinning and irregularity of the cribriform plates is seemingly present throughout the population, even in patients without CSF leaks. However, at our institution, we mention all focal defects in patients with proven leaks, particularly if there is adjacent soft tissue in the olfactory recess (Fig. 24).
- Particularly in the setting of IIH, the presence of multiple osseous defects and/or meningoceles complicates determining which site is currently leaking. CT or MR cisternograms can be helpful in this setting, but occasionally these are negative if the patient is not leaking at the time of imaging. In these cases, the surgeons often stage the repairs, and address the site that is considered most suspicious first.
- CTC in the postoperative setting, particularly in the setting of a recurrent leak, is challenging, because osteoneogenesis, inspissated secretions, and postoperative graft/granulation tissue are all increased in density. Thus, it is imperative to review precontrast and postcontrast images side by side. Soft tissue algorithm images can be helpful in assessing density differences (Fig. 25).
- Drawing ROIs in the mastoid air cells or other small variant cells on CTC can be difficult. Magnifying the images can help, but occasionally it is impossible.
- Occasionally, particularly in the setting of IIH, meningoceles can present with a canal-like appearance, with linear tracts extending through the bone. It is important to delineate the entire course of the meningocele to minimize the potential for recurrence, which can be done via a combination of thin section T2w MR cisternograms and CT (Fig. 26).

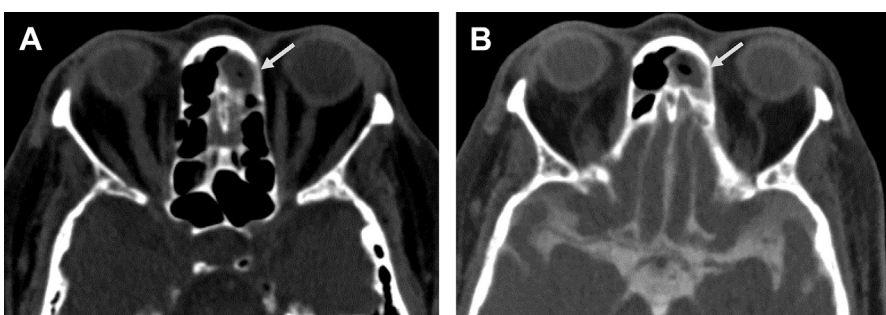


Fig. 25. Pitfall: CT cisternogram in the postoperative setting can be challenging because of underlying osteoneogenesis, as in this patient with recurrent leak after repair of a left frontal sinus meningocele. Comparing the pre-contrast (A) and postcontrast (B) images shows only peripheral osteoneogenesis in the left frontal sinus (arrows), without definite leak at the postoperative site. Optimizing window and level settings on soft tissue windows is often helpful.

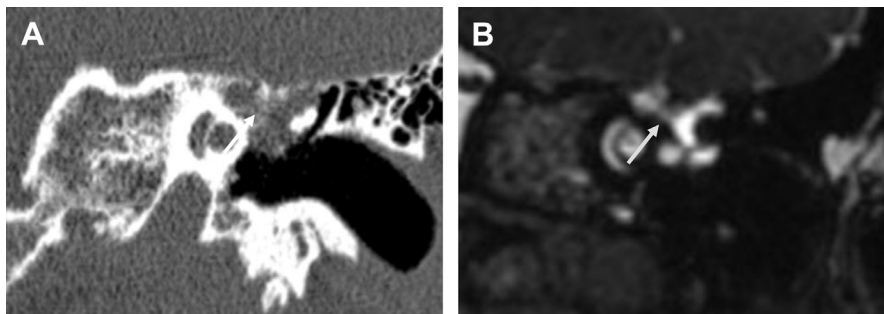


Fig. 26. Pitfall: meningoceles can be multifocal and present with a canal-like appearance, particularly in the setting of IIH, with linear tracts connecting different areas of meningoceles, as in this patient with a meningocele in the left middle ear, medial to ossicles seen on Coronal temporal bone CT (A) and T2w MRI images (B). This meningocele communicated via a tract to the region of the geniculate ganglion (arrows), a finding that was confirmed intraoperatively. Identifying the entire course of the meningocele is important to minimize the potential for recurrence postoperatively.

- Performing lumbar punctures for cisternography on obese patients (commonly encountered in IIH) may be technically challenging. A standard-length 89-mm (3.5-inch) spinal needle is used to access the thecal sac in most patients. In obese patients, 127-mm (5-inch) and 178-mm (7-inch) needles may be needed; however, these can become difficult to steer. In these cases, clinicians can use an 18-gauge 89-mm needle to guide the longer needle using a coaxial technique.

WHAT SURGEONS WANT TO KNOW

All of the following information should be included in the imaging reports of these patients, if possible:

- Location and size of defects measured in multiple planes; scrutinize entire skull base, including sinuses and mastoids.
- Anatomy of sinonasal cavity (ie, nasal septal deviation, perforation, variants) for surgical planning/approach.
- Presence of associated meningoencephaloceles (may need MR cisternogram).
- Presence of imaging features suggestive of underlying IIH.
- Sites that are actively leaking.
- Entire course of meningocele tract (heavily T2w images and CT).
- Opening pressure, if performing cisternography. However, keep in mind that it is common for the opening pressure to be normal or only borderline increased in patients with IIH in the setting of an ongoing leak.

SUMMARY

The work-up of CSF rhinorrhea and otorrhea can be complex, often requiring a time-intensive and

labor-intensive thorough investigation of the skull base on multiple modalities. It is important to have an algorithm for the approach to this challenging clinical problem, to be aware of potential pitfalls in imaging these patients, and to focus on what surgeons need to know to guide appropriate surgical planning.

REFERENCES

1. Daudia A, Biswas D, Jones NS. Risk of meningitis with cerebrospinal fluid rhinorrhea. Ann Otol Rhinol Laryngol 2007;116(12):902–5.
2. Miner JR, Heegaard W, Mapes A, et al. Presentation, time to antibiotics, and mortality of patients with bacterial meningitis at an urban county medical center. J Emerg Med 2001;21(4):387–92.
3. Komotar RJ, Starke RM, Raper D, et al. Endoscopic endonasal versus open repair of anterior skull base CSF leak, meningocele, and encephalocele: a systematic review of outcomes. J Neurol Surg A Cent Eur Neurosurg 2013;74(4):239–50.
4. Sharma S, Kumar G, Bal J, et al. Endoscopic repair of cerebrospinal fluid rhinorrhoea. Eur Ann Otorhinolaryngol Head Neck Dis 2016;133(3):187–90.
5. Locatelli D, Rampa F, Acchiardi I, et al. Endoscopic endonasal approaches for repair of cerebrospinal fluid leaks: nine-year experience. Neurosurgery 2006;58(4):ONS-246–56.
6. Ommaya AK, Di Chiro G, Baldwin M, et al. Non-traumatic cerebrospinal fluid rhinorrhea. J Neurol Neurosurg Psychiatr 1968;31(3):214–25.
7. Schlosser RJ, Wilensky EM, Grady MS, et al. Elevated intracranial pressures in spontaneous cerebrospinal fluid leaks. Am J Rhinol 2003;17:191–5.
8. Oakley GM, Alt JA, Schlosser RJ, et al. Diagnosis of cerebrospinal fluid rhinorrhea: an evidence-based review with recommendations. Int Forum Allergy Rhinol 2016;6:8–16.

9. McCudden CR, Senior BA, Hainsworth S, et al. Evaluation of high resolution gel β 2-transferrin for detection of cerebrospinal fluid leak. *Clin Chem Lab Med* 2013;51(2):311–5.
10. Bleier BS, Debnath I, O'Connell BP, et al. Preliminary study on the stability of beta-2 transferrin in extracorporeal cerebrospinal fluid. *Otolaryngol Head Neck Surg* 2011;144(1):101–3.
11. Schnabel C, Di Martino E, Gilsbach JM, et al. Comparison of β 2-transferrin and β -trace protein for detection of cerebrospinal fluid in nasal and ear fluids. *Clin Chem* 2004;50(3):661–3.
12. Arrer E, Meco C, Oberascher G, et al. β -Trace protein as a marker for cerebrospinal fluid rhinorrhea. *Clin Chem* 2002;48(6):939–41.
13. Mostafa BE, Khafagi A. Combined HRCT and MRI in the detection of CSF rhinorrhea. *Skull Base* 2004; 14(3):157–61.
14. Algin O, Hakyemez B, Gokalp G, et al. The contribution of 3D-CISS and contrast-enhanced MR cisternography in detecting cerebrospinal fluid leak in patients with rhinorrhoea. *Br J Radiol* 2014; 83(987):225–32.
15. Zapalac JS, Marple BF, Schwade ND. Skull base cerebrospinal fluid fistulas: a comprehensive diagnostic algorithm. *Otolaryngol Head Neck Surg* 2002;126(6):669–76.
16. Shetty PG, Shroff MM, Sahani DV, et al. Evaluation of high-resolution CT and MR cisternography in the diagnosis of cerebrospinal fluid fistula. *AJNR Am J Neuroradiol* 1998;19(4):633–9.
17. La Fata V, McLean N, Wise S, et al. CSF leaks: correlation of high-resolution CT and multiplanar reformations with intraoperative endoscopic findings. *AJNR Am J Neuroradiol* 2008;29(3):536–41.
18. Zuckerman JD, DelGaudio JM. Utility of preoperative high-resolution CT and intraoperative image guidance in identification of cerebrospinal fluid leaks for endoscopic repair. *Am J Rhinol* 2008;22(2):151–4.
19. Schuknecht B, Simmen D, Briner H, et al. Nontraumatic skull base defects with spontaneous CSF rhinorrhea and arachnoid herniation: imaging findings and correlation with endoscopic sinus surgery in 27 patients. *AJNR Am J Neuroradiol* 2008;29(3):542–9.
20. Lloyd KM, DelGaudio JM, Hudgins PA. Imaging of skull base cerebrospinal fluid leaks in adults. *Radiology* 2008;248(3):725–36.
21. Drayer BP, Wilkins RH, Boehnke M, et al. Cerebrospinal fluid rhinorrhea demonstrated by metrizamide CT cisternography. *AJR Am J Roentgenol* 1977; 129(1):149–51.
22. Vimla LR, Jasper A, Irodi A. Non-invasive and minimally invasive imaging evaluation of CSF rhinorrhoea - a retrospective study with review of literature. *Pol J Radiol* 2016;81:80–5.
23. Stone JA, Castillo M, Neelon B, et al. Evaluation of CSF leaks: high-resolution CT compared with contrast-enhanced CT and radionuclide cisternography. *AJNR Am J Neuroradiol* 1999;20(4):706–12.
24. Tahir MZ, Khan MB, Bashir MU, et al. Cerebrospinal fluid rhinorrhea: an institutional perspective from Pakistan. *Surg Neurol Int* 2011;2:174.
25. Goel G, Ravishankar S, Jayakumar P, et al. Intra-thecal gadolinium-enhanced magnetic resonance cisternography in cerebrospinal fluid rhinorrhea: road ahead? *J Neurotrauma* 2007;24(10):1570–5.
26. Chow JM, Goodman D, Mafee MF. Evaluation of CSF rhinorrhea by computerized tomography with metrizamide. *Otolaryngol Head Neck Surg* 1989;100(2): 99–105.
27. Tuntiyatorn L, Laothammatas J. Evaluation of MR cisternography in diagnosis of cerebrospinal fluid fistula. *J Med Assoc Thai* 2004;87(12):1471–6.
28. Rajeswaran R, Chandrasekharan A, Mohanty S, et al. Role of MR cisternography in the diagnosis of cerebrospinal fluid rhinorrhoea with diagnostic nasal endoscopy and surgical correlation. *Indian J Radiol Imaging* 2006;16(3):315.
29. Ragheb AS, Mohammed FF, El-Anwar MW. Cerebrospinal fluid rhinorrhea: diagnostic role of gadolinium enhanced MR cisternography. *The Egyptian Journal of Radiology and Nuclear Medicine* 2014;45(3):841–7.
30. Delgaudio JM, Baugnon KL, Wise SK, et al. Magnetic resonance cisternogram with intrathecal gadolinium with delayed imaging for difficult to diagnose cerebrospinal fluid leaks of the anterior skull base. *Int Forum Allergy Rhinol* 2015;5(4):333–8.
31. Selcuk H, Albayram S, Ozer H, et al. Intrathecal gadolinium-enhanced MR cisternography in the evaluation of CSF leakage. *AJNR Am J Neuroradiol* 2010;31(1):71–5.
32. Aydin K, Terzibasioglu E, Sencer S, et al. Localization of cerebrospinal fluid leaks by gadolinium-enhanced magnetic resonance cisternography: a 5-year single-center experience. *Neurosurgery* 2008;62(3):584–9.
33. Arbeláez A, Medina E, Rodríguez M, et al. Intra-thecal administration of gadopentetate dimeglumine for MR cisternography of nasoethmoidal CSF fistula. *AJR Am J Roentgenol* 2007;188(6):W560–4.
34. Vanhee A, Dedeken P, Casselman J, et al. MRI with intrathecal gadolinium to detect a CSF leak: feasibility and long term safety from an open label single centre cohort study. *Neurology* 2016;86(16 Suppl P4):113.
35. Dillon WP. Intrathecal gadolinium: its time has come? *AJNR Am J Neuroradiol* 2008;29:3–4.
36. Zlab MK, Moore GF, Daly DT, et al. Cerebrospinal fluid rhinorrhea: a review of the literature. *Ear Nose Throat J* 1992;71(7):314–7.
37. Baugnon KL, Hudgins PA. Skull base fractures and their complications. *Neuroimaging Clin N Am* 2014; 24(3):439–65.
38. Schlosser RJ, Bolger WE. Nasal cerebrospinal fluid leaks: critical review and surgical considerations. *Laryngoscope* 2004;114:255–65.

39. Bell RB, Dierks EJ, Homer L, et al. Management of cerebrospinal fluid leak associated with craniomaxillofacial trauma. *J Oral Maxillofac Surg* 2004;62(6):676–84.
40. Eljamal MS, Foy PM. Acute traumatic CSF fistulae: the risk of intracranial infection. *Br J Neurosurg* 1990;4:381–5.
41. Lloyd MN, Kimber PM, Burrows EH. Post-traumatic CSF rhinorrhea: modern HRCT is all that is required for the effective demonstration of the site of leakage. *Clin Radiol* 1994;49:100–3.
42. Platt MP, Parnes SM. Management of unexpected cerebrospinal fluid leak during endoscopic sinus surgery. *Curr Opin Otolaryngol Head Neck Surg* 2009;17:28–32.
43. Naunheim MR, Sedaghat AR, Lin DT, et al. Immediate and delayed complications following endoscopic skull base surgery. *J Neurol Surg B Skull Base* 2015;76(5):390–6.
44. Ota N, Tanikawa R, Miyazaki T, et al. Surgical microanatomy of the anterior clinoid process for paraclinoid aneurysm surgery and efficient modification of extradural anterior clinoidectomy. *World Neurosurg* 2015;83(4):635–43.
45. Spektor S, Dotan S, Mizrahi CJ. Safety of drilling for clinoidectomy and optic canal unroofing in anterior skull base surgery. *Acta Neurochir* 2013;155(6):1017–24.
46. Batier HH, Welch BG. Respecting the clinoid: an application of preoperative computed tomography angiography. *World Neurosurg* 2015;83(6):1022–3.
47. Bumm K, Heupel J, Bozzato A, et al. Localization and infliction pattern of iatrogenic skull base defects following endoscopic sinus surgery at a teaching hospital. *Auris Nasus Larynx* 2009;36:671–6.
48. Yadav YR, Parihar V, Janakiram N, et al. Endoscopic management of cerebrospinal fluid rhinorrhea. *Asian J Neurosurg* 2016;11(3):183–93.
49. Durcan PJ, Corbett JJ, Wall M. The incidence of pseudotumor cerebri: population studies in Iowa and Louisiana. *Arch Neurol* 1988;45(8):875–7.
50. O'Connell B, Stevens S, Xiao C, et al. Lateral skull base attenuation in patients with anterior cranial fossa spontaneous cerebrospinal fluid leaks. *Otolaryngol Head Neck Surg* 2016;154(6):1138–44.
51. Wang EW, Vandergrift WA, Schlosser RJ. Spontaneous CSF leaks. *Otolaryngol Clin North Am* 2011;44(4):845–56.
52. Tabaei A, Kassenoff TL, Kacker A, et al. The efficacy of computer assisted surgery in the endoscopic management of cerebrospinal fluid rhinorrhea. *Otolaryngol Head Neck Surg* 2005;133(6):936–43.
53. Banks CA, Palmer JN, Chiu AG, et al. Endoscopic closure of CSF rhinorrhea: 193 cases over 21 years. *Otolaryngol Head Neck Surg* 2009;140(6):826–33.
54. Bidot S, Saindane AM, Peragallo JH, et al. Brain imaging in idiopathic intracranial hypertension. *J Neuroophthalmol* 2015;35(4):400–11.
55. Settecasse F, Harnsberger HR, Michel MA, et al. Spontaneous lateral sphenoid cephaloceles: anatomic factors contributing to pathogenesis and proposed classification. *AJNR Am J Neuroradiol* 2014;35:784–9.
56. Bialer OY, Rueda MP, Bruce BB, et al. Meningoceles in idiopathic intracranial hypertension. *AJR Am J Roentgenol* 2014;202(3):608.
57. Aiken AH, Hoots J, Saindane A, et al. Incidence of cerebellar tonsillar ectopia in idiopathic intracranial hypertension: a mimic of the Chiari I malformation. *AJNR Am J Neuroradiol* 2012;33(10):1901–6.
58. Mishara S, Mathew G, Paul R, et al. Endoscopic repair of CSF rhinorrhea: an institutional experience. *Iran J Otorhinolaryngol* 2016;28(84):39–43.
59. Clark D, Bullock P, Hui T, et al. Benign intracranial hypertension: a cause of CSF rhinorrhoea. *J Neurol Neurosurg Psychiatr* 1994;57(7):847–9.
60. Shetty PG, Shroff MM, Fatterpekar GM, et al. A retrospective analysis of spontaneous sphenoid sinus fistula: MR and CT findings. *AJNR Am J Neuroradiol* 2000;21(2):337–42.
61. Schlosser RJ, Bolger WE. Management of multiple spontaneous nasal meningoencephaloceles. *Laryngoscope* 2002;112(6):980–5.
62. Hubbard JL, McDonald TJ, Pearson BW, et al. Spontaneous cerebrospinal fluid rhinorrhea: evolving concepts in diagnosis and surgical management based on the Mayo Clinic experience from 1970 through 1981. *Neurosurgery* 1985;16:314–21.
63. Schick B, Ibing R, Brors D, et al. Long term study of endonasal duraplasty and review of the literature. *Ann Otol Rhinol Laryngol* 2001;110:142–7.
64. Gassner HG, Ponikau JU, Sherris DA, et al. CSF rhinorrhea: 95 consecutive surgical cases with long term follow-up at the Mayo Clinic. *Am J Rhinol* 1999;13:439–47.
65. Chaaban MR, Illing E, Riley KO, et al. Spontaneous cerebrospinal fluid leak repair: a five year prospective evaluation. *Laryngoscope* 2014;124(1):70–5.
66. Keerl R, Weber RK, Draf W, et al. Use of sodium fluorescein solution for detection of cerebrospinal fluid fistulas: an analysis of 420 administrations and reported complications in Europe and the United States. *Laryngoscope* 2004;114:266–72.
67. Manes RP, Ryan MW, Marple BF. A novel finding on CT in the diagnosis and localization of CSF leaks without a clear bony defect. *Int Forum Allergy Rhinol* 2012;2(5):402–4.
68. Schwartz KM, Lane JI, Bolster BD Jr, et al. The utility of diffusion weighted imaging for cholesteatoma evaluation. *AJNR Am J Neuroradiol* 2011;32:430–6.
69. Abele TA, Salzman KL, Harnsberger HR, et al. Craniopharyngeal canal and its spectrum of pathology. *Am J Neuroradiol* 2014;35(4):772–7.